Quantitative phosphoproteomic analysis reveals cAMP/vasopressin-dependent signaling pathways in native renal thick ascending limb cells

Ruwan Gunaratne, Drew W. W. Braucht, Markus M. Rinschen, Chung-Lin Chou, Jason D. Hoffert, Trairak Pisitkun, and Mark A. Knepper[1]

Epithelial Systems Biology Laboratory, National Heart, Lung and Blood Institute, National Institutes of Health, Bethesda, MD 20892

Edited* by Peter Agre, Johns Hopkins Malaria Research Institute, Baltimore, MD, and approved July 20, 2010 (received for review May 27, 2010)

Quantitative mass spectrometry was used to identify hormone-dependent signaling pathways in renal medullary thick ascending limb (mTAL) cells via phosphoproteomic analysis. Active transport of NaCl across the mTAL epithelium is accelerated by hormones that increase cAMP levels (vasopressin, glucagon, parathyroid hormone, and calcitonin). mTAL suspensions from rat kidneys were exposed (15 min) to a mixture of these four hormones. Tryptic phosphopeptides (immobilized metal affinity chromatography-enriched) were identified and quantified by mass spectrometry (LTQ-Orbitrap) using label-free methodology. We quantified a total of 654 phosphopeptides, of which 414 were quantified in three experimental pairs (hormone vs. vehicle). Of these phosphopeptides, 82% were statistically unchanged in abundance in response to the hormone mixture. In contrast, 48 phosphopeptides were significantly increased, whereas 28 were significantly decreased. The population of up-regulated phosphopeptides was highly enriched in basophilic kinase substrate motifs (AGC or calmodulin-sensitive kinase families), whereas the down-regulated sites were dominated by "proline-directed" motifs (cyclin-dependent or MAP kinase families). Bioinformatic classification uncovered overrepresentation of transmembrane transporters, protein phosphatase regulators, and cytoskeletal binding proteins among the regulated proteins. Immunoblotting with phospho-specific antibodies confirmed cAMP/vasopressin-dependent phosphorylation at Thr96, Ser126, and Ser874 of the Na^+:K^+:$2Cl^-$ cotransporter NKCC2, at Ser552 of the Na^+:H^+ exchanger NHE3, and at Ser552 of β-catenin. Vasopressin also increased phosphorylation of NKCC2 at both Ser126 (more than fivefold) and Ser874 (more than threefold) in rats in vivo. Both sites were phosphorylated by purified protein kinase A during in vitro assays. These results support the view that, although protein kinase A plays a central role in mTAL signaling, additional kinases, including those that target proline-directed motifs, may be involved.

protein phosphatase | glucose transporters | mass spectrometry | ion transporters | protein kinase

The thick ascending limb (TAL) of Henle's loop is a nephron segment that plays a critical role in the control of mammalian water excretion. Active NaCl transport by the medullary TAL (mTAL) drives the countercurrent multiplication process that concentrates the urine (1). Hormones that increase the concentration of the intracellular second messenger, cAMP, have been shown to enhance the rate of NaCl transport in mTAL cells (2). These hormones include parathyroid hormone (PTH), calcitonin, glucagon, and vasopressin (2). Among these, only vasopressin plays a selective role in regulation of water balance. The molecular targets for cAMP-mediated regulation in the mTAL include the apical Na^+:K^+:$2Cl^-$ cotransporter NKCC2 (gene symbol: *Slc12a1*) and the apical Na^+:H^+ exchanger NHE3 (*Slc9a3*) (3).The signaling network that accounts for cAMP-dependent regulation of these transporters is largely unknown but critical to understanding the cellular physiology of the mTAL.

Virtually all cell signaling processes are dependent on protein phosphorylation and dephosphorylation. To discover the key elements of cAMP-mediated cell signaling in the mTAL, in this study we have carried out large-scale liquid chromatography tandem mass spectrometry (LC-MS/MS)-based phosphoproteomic profiling and quantification in native mTAL cell suspensions isolated from rat kidneys. We quantified changes in mTAL protein phosphorylation in response to hormones that increase cAMP, including vasopressin. The findings include regulated phosphorylation sites in several key transporters.

Results

Technical Controls. Volumetrically, the mTAL is the dominant structure in the renal outer medulla (4). mTAL suspensions showed further enrichment of the TAL marker protein NKCC2 with respect to the whole outer medulla, although residual amounts of the collecting duct water channel AQP2 and the descending limb water channel AQP1 were present (Fig. S1). Intracellular cAMP increased in these mTAL suspensions (Fig. 1) upon stimulation with glucagon, PTH, calcitonin, and/or the V_2 receptor-selective vasopressin analog dDAVP [using hormone concentrations culled from previous studies (*SI Materials and Methods*)]. Because the mixture of all four hormones (in the presence of phosphodiesterase inhibitor IBMX) induced the largest cAMP response, this combination was used for mass spectrometry (MS)-based profiling and quantification of the mTAL phosphoproteome.

Phosphoproteomic Profiling, Quantification, and Bioinformatic Analysis. mTAL suspensions exposed to the hormone mixture (dDAVP, glucagon, PTH, and calcitonin in the presence of 0.5 mM IBMX) or to the vehicle (no hormones or IBMX) were processed for LC-MS/MS-based phosphoproteomic analysis ($n = 3$). After denaturation in 8 M urea followed by trypsinization, Ga^{3+}-immobilized metal affinity chromatography (IMAC) was used to enrich phosphopeptides. The MS spectra (LTQ-Orbitrap) were matched to specific peptide sequences using three search algorithms (SEQUEST, InSPecT, and OMSSA), adjusting search parameters based on target-decoy analysis (5) to limit the false discovery rate to <2%. Each of the three search algorithms added a significant number of identifications (Fig. 2 *A* and *B*). A total of 654 unique phosphopeptides was identified corresponding to 374 unique proteins (Table S1). The data were used to populate a publicly available database, which can be accessed at http://dir.nhlbi.nih.gov/papers/lkem/mtalpd/.

The relative abundance of each phosphopeptide was quantified as the area under its MS^1-time-course curve. Fig. 2*C* shows a histogram of the hormone:vehicle abundance ratios for the 414

Author contributions: R.G., J.D.H., T.P., and M.A.K. designed research; R.G., D.W.W.B., M.M.R., C.-L.C., and T.P. performed research; J.D.H. and T.P. contributed new reagents/analytic tools; R.G., D.W.W.B., M.M.R., T.P., and M.A.K. analyzed data; R.G., D.W.W.B., T.P., and M.A.K. wrote the paper.

The authors declare no conflict of interest.

*This Direct Submission article had a prearranged editor.

Data deposition: Mass spectrometry data have been deposited in the Tranche Repository (http://www.proteomecommons.org/) (hash: F+7Jv1/Py0TMAp5w+spCDGMMJ06Ki965Ad1rsc0DVk457/LxujZziDhPKcYKUst960wKR+Jlsfv55OAG0caHw0l8d8oAAAAAAAAHsQ==).

[1]To whom correspondence should be addressed. E-mail: knepperm@nhlbi.nih.gov.

This article contains supporting information online at www.pnas.org/lookup/suppl/doi:10.1073/pnas.1007424107/-/DCSupplemental.

SYSTEMS BIOLOGY

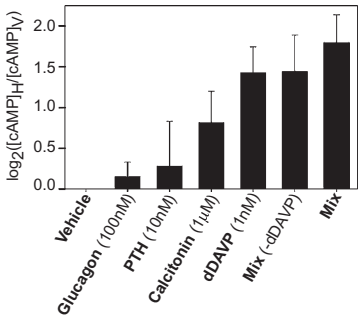

Fig. 1. Cellular cAMP following hormone stimulation. Measurements made in presence of IBMX (0.5 mM). dDAVP is a V2-receptor selective vasopressin analog. Error bars indicate SEM (n = 3).

phosphopeptides that were quantified in all three experimental pairs. Although the majority of the phosphopeptides showed no change in phosphorylation state in response to the hormone mixture, 48 peptides were significantly increased (Fig. 2*C*, blue) whereas 28 peptides were significantly decreased (Fig. 2*C*, red). These 76 regulated phosphopeptides correspond to 56 different proteins. The subset of regulated phosphorylation sites from those phosphopeptides whose ratios exceeded $|\log_2[\text{hormone/vehicle}]| > 0.58$ are presented in Table 1 (increased) and Table 2 (decreased). The complete list of regulated phosphorylation sites can be found in Table S1 or at http://dir.nhlbi.nih.gov/papers/lkem/mtalpd/.

To identify linear substrate motifs for kinases activated and inactivated in response to the cAMP-generating hormone mixture, sequence logos were constructed from aligned sequences of the up- and down-regulated peptides using the web tool *enoLOGOS* (6). Fig. 2*D* summarizes the statistically overrepresented target

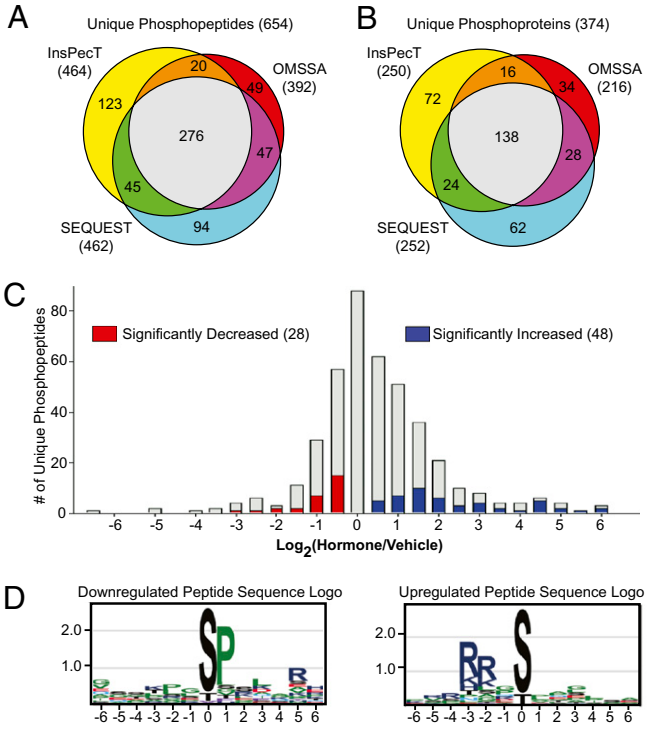

Fig. 2. Phosphoproteomic profiling summary. Phosphopeptides (*A*) and corresponding phosphoproteins (*B*) identified by each search engine (SEQUEST, InsPecT, and OMSSA). (*C*) Distribution of changes in abundance of individual phosphorylation sites in response to hormone treatment (significantly decreased, red; significantly increased, blue). (*D*) Amino acid residue/position pairs overrepresented in sets of phosphopeptides whose abundances are significantly decreased (*Left*) or significantly increased (*Right*).

sequences. The information content at each position in the sequence logo is reflected by the total height of its letter stack (measured in bits), whereas the probability of observing a certain amino acid relative to its proteome-wide frequency is proportional to its size at each position. Analysis of the up-regulated phosphopeptides revealed a preference for basic amino acids in the −2 and −3 positions, typical of substrates for basophilic kinases in the A, G and C (AGC) kinase and calmodulin-sensitive kinase (CAMK) families (7). In contrast, analysis of the down-regulated peptides showed a strong predilection for a proline residue at the +1 position, a hallmark of substrates for proline-directed kinases such as MAP kinases and cyclin-dependent kinases (7).

We asked whether certain classes of proteins are overrepresented among the regulated phosphoproteins by using the DAVID bioinformatic tool [Database for Annotation, Visualization, and Integrated Discovery, http://david.abcc.ncifcrf.gov/ (8)]. The control dataset was the list of all mTAL-expressed genes [mTAL Transcriptome Database, http://dir.nhlbi.nih.gov/papers/lkem/mtaltr/ (9)]. The molecular function Gene Ontology terms that were statistically significantly enriched ($P < 0.05$, Fisher's exact test) were "transmembrane transporters," "protein phosphatase regulators," and "cytoskeletal binding proteins." The "transmembrane transporters" included up-regulated sites in NKCC2 (*Slc12a1* at Thr96, Ser126, Ser874), NHE3 (*Slc9a3* at Ser552), the insulin-sensitive facilitated glucose transporter Glut4 (*Slc2a4* at Ser488), and the neutral amino acid transporter Lat4 (*Slc43a2* at Ser274). The "protein phosphatase regulators" (i.e., phosphatase regulatory subunits) were *Ppp1r1b* (DARPP32), *Ppp1r1a*, and *Ppp2r5d*. An additional phosphatase regulator, tensin (*Tns*), exhibited numerous regulated phosphorylation sites (Tables 1 and 2). The other overrepresented functional category, "cytoskeletal binding proteins," included tensin, BIG2 (*Arfgef2*), drebrin-like protein (*Dbnl*), and paxillin (*Pxn*).

Confirmation of Regulated Phosphorylation Sites in NKCC2, NHE3, and β-Catenin. Two phosphorylation sites in the Na^+:K^+:$2Cl^-$ cotransporter, NKCC2, were strongly up-regulated by cAMP-increasing hormones, i.e., at a previously unreported site at Ser874 and a known site at Ser126 (10). MS^3 spectra for Ser126 (Fig. 3*A*) and Ser874 (Fig. 3*B*) allowed unambiguous site assignments. The corresponding MS^1 time-course curves showed increased phosphorylation upon hormone treatment. Both sites are compatible with phosphorylation by so-called "basophilic kinases" with basic amino acids (R or K) at positions −2 and/or −3 upstream from the targeted serine. Fig. 3*C* shows an MS^2 spectrum and MS^1 time-course curves for another identified NKCC2 monophosphopeptide that was also up-regulated in response to the hormone mixture. This peptide spans two previously demonstrated phosphorylation sites (Thr96 and Thr101) (11), but the spectra for this peptide did not allow definitive localization of the modified threonine. Immunoblotting of paired vehicle- and hormone-treated mTAL suspensions with an antibody (R5) that targets doubly phosphorylated (Thr96/Thr101) NKCC2 (11) confirmed an increase in phosphorylation (Fig. 3*D*, *Top* blot). To identify the site responsible for the change, the R5 antibody was preadsorbed with synthetic peptides singly phosphorylated at either Thr96 or Thr101 and used for immunoblotting (Fig. 3*D*). Although the Thr101 site did not change significantly upon hormone treatment, the density of the band corresponding to phosphorylation at Thr96 was increased by nearly twofold [hormone/vehicle (H/V) ratio: 1.7 ± 0.4 (SE), $P < 0.05$], establishing Thr96 as the regulated site (Fig. 3*D*, bar graph).

We raised rabbit polyclonal phospho-specific antibodies against NKCC2 phosphorylated at Ser126 or Ser874. Dot blotting verified the specificity of both NKCC2 phospho-antibodies (Fig. S2). Immunoblotting with these antibodies confirmed strong increases in phosphorylation at both Ser126 (H/V ratio: 38.5 ± 4.7, $P < 0.05$) and Ser874 (H/V ratio: 4.2 ± 1.0, $P < 0.05$) in response to the hormone mixture (Fig. 4*A*). Similar responses were seen upon treatment of mTAL suspensions with the vasopressin analog dDAVP alone at 1 nM (Fig. S3).

The up-regulated phosphorylation sites uncovered by MS also included Ser552 of NHE3 and Ser552 of β-catenin. Fig. 4 *B* and *C* show immunoblotting with phospho-specific antibodies to both of these sites. The cAMP-generating hormone mixture increased phosphorylation of NHE3 at Ser552 (H/V ratio: 1.8 ± 0.2, $P < 0.05$)

Table 1. Phosphorylation sites of quantified phosphopeptides that increased in abundance in response to the cAMP-generating hormone mixture (n = 3)

Gene symbol	Phosphorylation site(s)	$\log_2$(H/V) (mean ± SE)
Ppp1r1b (DARPP32)	Thr34	6.20 ± 0.49
Slc12a1 (NKCC2)	Ser126	5.90 ± 0.24
Rap1ga1	Ser505	5.36 ± 0.67
Rap1ga1	Ser557,Ser574	4.98 ± 0.66
Fam54b	Ser38	4.83 ± 0.60
Sec22b	Ser137	4.74 ± 0.77
Smpx	Ser36	4.47 ± 0.42
Smpx	Thr40	4.47 ± 0.42
Card14	Thr278*	4.47 ± 0.42
Lrba	Ser898	4.45 ± 0.17
Sort1	Ser791	3.87 ± 0.46
St14	Ser13	3.73 ± 0.86
Snx3	Ser72	3.47 ± 0.34
Cgnl1	Thr258, Ser261	3.19 ± 0.74
Slc12a1 (NKCC2)	Ser874	3.05 ± 0.71
Eplin	Ser132	2.88 ± 0.51
Cgnl1	Ser256, Ser261	2.87 ± 0.56
Ank3	Thr2465	2.64 ± 0.45
Kif26a	Ser942	2.42 ± 0.53
Rap1ga1	Ser589	2.40 ± 0.30
Ctnnb1 (β-catenin)	Ser552†	2.15 ± 0.15
Ppp2r5d	Ser632	2.11 ± 0.46
Rbm14	Ser618	2.10 ± 0.24
Slc9a3 (NHE3)	Ser552	2.07 ± 0.30
Ctnnb1 (β-catenin)	Ser552†	2.04 ± 0.46
Ctnnb1 (β-catenin)	Thr551*	2.04 ± 0.46
Aqp2	Ser256†	1.70 ± 0.24
Plxdc2	Ser507	1.69 ± 0.32
Aqp2	Ser256†	1.60 ± 0.17
Ppp1r1a	Thr35	1.53 ± 0.20
Pum1	Ser710	1.52 ± 0.13
Ndrg2	Thr316*	1.52 ± 0.30
Plekha6	Ser1094	1.45 ± 0.17
Cyba	Ser168	1.34 ± 0.26
Mme	Ser4	1.31 ± 0.17
Slc12a1 (NKCC2)	Thr96	1.31 ± 0.23
Phldb2	Ser510	1.22 ± 0.17
Fam82a2	Ser44	1.18 ± 0.06
Tns (tensin)	Ser628	1.17 ± 0.25
Pxn (paxillin)	Ser315	1.00 ± 0.19
Slc2a4 (Glut4)	Ser488*	0.97 ± 0.22
Slc43a2 (Lat4)	Ser274	0.88 ± 0.18
Ank3	Ser1458	0.88 ± 0.20
Golgb1	Ser614	0.64 ± 0.05
Gng12	Ser49	0.63 ± 0.14

H, hormone treated; V, vehicle.
*Ambiguous phosphorylation site assignment.
†Site quantified in multiple phosphopeptides.

Table 2. Quantified phosphopeptides that decreased in abundance in response to the cAMP-generating hormone mixture (n = 3)

Gene symbol	Phosphorylation site(s)	$\log_2$(H/V) (mean ± SE)
Tns (tensin)	Ser1523†	−2.89 ± 0.60
Tns (tensin)	Ser1497*	−2.34 ± 0.28
Tns (tensin)	Ser1467	−2.04 ± 0.06
Tns (tensin)	Ser1523†	−2.02 ± 0.28
Slc43a2 (Lat4)	Ser297	−1.50 ± 0.16
Eif4b	Ser459	−1.35 ± 0.07
Sec61b	Ser17	−1.09 ± 0.25
Palm	Thr145	−1.09 ± 0.17
Esam	Ser348	−1.08 ± 0.20
Tns (tensin)	Thr1582	−0.98 ± 0.12
Arfgef2 (BIG2)	Ser218, Ser227	−0.90 ± 0.12
Tns (tensin)	Ser1568	−0.86 ± 0.15
Disc1	Ser623,* Ser631*	−0.77 ± 0.17
Lmna	Ser389	−0.74 ± 0.17
Add3	Ser648	−0.73 ± 0.16
Tns (tensin)	Ser1446	−0.68 ± 0.16
Ahnak	Ser2257	−0.67 ± 0.15
Tjp2	Ser107	−0.62 ± 0.13

H, hormone treated; V, vehicle.
*Ambiguous phosphorylation site assignment.
†Site quantified in multiple phosphopeptides.

and β-catenin at Ser552 (H/V ratio: 3.9 ± 0.5, $P < 0.05$) in mTAL suspensions, confirming the MS results. NHE3 phosphorylation at Ser552 was similarly increased in response to dDAVP alone (Fig. S4).

Vasopressin Increases NKCC2 Phosphorylation at Ser126 and Ser874 in Vivo. Intramuscular injection with dDAVP in Brattleboro rats, which lack endogenous vasopressin, led to significant increases in phosphorylation at both Ser126 and Ser874 as revealed by immunoblotting of outer medullary homogenates (H/V ratio: 5.2 ± 1.0, $P < 0.05$, for p-Ser126; H/V ratio: 3.2 ± 0.3, $P < 0.05$, for p-Ser874) (Fig. 5*A*). Confocal immunofluorescence of fixed and embedded Brattleboro rat kidneys showed phosphorylated NKCC2 labeling limited to the apical region of thick ascending limb cells (Fig. 5 *B* and *C*). Phosphorylated NKCC2 labeling was seen only in kidneys from dDAVP-treated animals and was notably heterogeneous in distribution (compared with total NKCC2 distribution).

Phosphorylation of NKCC2 Synthetic Peptides by Protein Kinase A and AMP-Activated Kinase in Vitro. Although other basophilic kinases are expressed in mTAL cells, protein kinase A (PKA) is a likely candidate for a role in cAMP-mediated signaling in the mTAL. To evaluate the ability of PKA to phosphorylate both NKCC2 sites, synthetic peptides corresponding to the nonphosphorylated form of each NKCC2 phosphorylation site were incubated with purified active PKA-α (*PRKACA*), and phosphorylation was assessed by LC-MS/MS and immunoblotting (Fig. 6). Because of previous evidence that Ser126 of NKCC2 may be a substrate for AMP-activated kinase (AMPK) (10), purified active AMPK (α2/β1/γ1 trimeric heterocomplex) was tested alongside PKA in this in vitro assay. Both detection methods established that PKA can strongly phosphorylate NKCC2 at either site. AMPK also phosphorylated Ser126, as well as its control peptide (Fig. S5). Note that the consensus substrate sequence reported for AMPK identifies a preference for methionine or leucine at the −5 position from the phosphorylated residue (7), a characteristic that is not shared by the sequence surrounding Ser126 of NKCC2. This may account for its lower ability to phosphorylate Ser126 compared with PKA.

Discussion

Here we present results from large-scale phosphoproteomic profiling and quantification in native renal mTAL epithelial cells. We examined the response to a mixture of hormones known to increase intracellular cAMP. The analysis identified 654 phosphopeptides, corresponding to 374 proteins. On the basis of statistical analysis of the 414 phosphopeptides quantified in all three experimental pairs, 76 showed significantly altered phosphorylation in response to the hormone mixture. According to our findings, we draw the following six conclusions: (A) The majority of sites at which phosphorylation increased were basophilic sites, which points to specific classes of kinases that may be activated. (B) The majority of sites at which phosphorylation decreased were proline-directed sites, which points to specific classes of kinases that may be deactivated. (C) Regulated phosphoproteins were predominantly those with the molecular functions "protein phosphatase regula-

SYSTEMS BIOLOGY

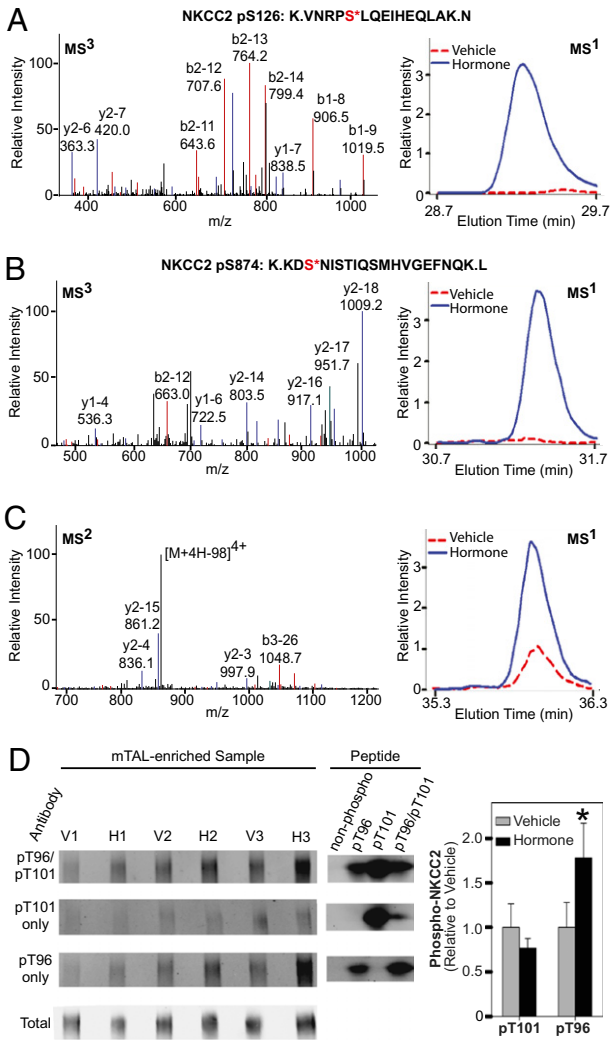

Fig. 3. NKCC2 phosphorylation. (*A*) pSer126-NKCC2 peptide. Typical MS^3 spectrum (*Left*) and representative MS^1 time-course curve (*Right*). (*B*) pSer874-NKCC2 peptide. (*C*) MS^2 spectrum (*Left*) for identified NKCC2 monophosphopeptide containing known phosphorylation sites at Thr96 and Thr101 (TDTTFHAYDSHTNTYYLQTFGHNTMDAVPK). Site specification cannot be determined. (*Right*) Representative MS^1 curves. (*D*) Immunoblots probed with R5 antibody (*Top*) or R5 antibody preadsorbed with synthetic peptides singly phosphorylated at either Thr96 or Thr101. (*Bottom*) "Total" immunoblot was probed with holo-NKCC2 antibody. (*Middle*) Controls in which synthetic phospho- and nonphospho-peptides were run on immunoblot and probed with designated antibodies. Bar graph shows results of densitometry analysis of immunoblots. H, hormone treated; V, vehicle. Error bars indicate SEM ($n = 3$). The asterisk indicates statistical significance ($P < 0.05$).

tion," "transmembrane transport," and "cytoskeletal binding." (D) Phosphorylation at two sites in the Na^+:K^+:$2Cl^-$ cotransporter NKCC2 (Ser126 and Ser874) is increased in response to vasopressin. (E) Phosphorylation at Ser552 in the sodium hydrogen exchanger NHE3 is increased in response to vasopressin. (F) A number of regulatory proteins were also phosphorylated or dephosphorylated in response to hormones that increase cAMP. In the remainder of the Discussion, we elaborate on these findings and relate them to the current literature.

Majority of Sites at Which Phosphorylation Increased Were Basophilic Sites. A basophilic site has basic amino acids (arginine, lysine, or histidine) in key positions surrounding the phosphorylated residue that determine the site specificity of phosphorylation. The basophilic pattern for up-regulated sites suggests that cAMP-mediated signaling in the mTAL involves regulation of kinases in the AGC

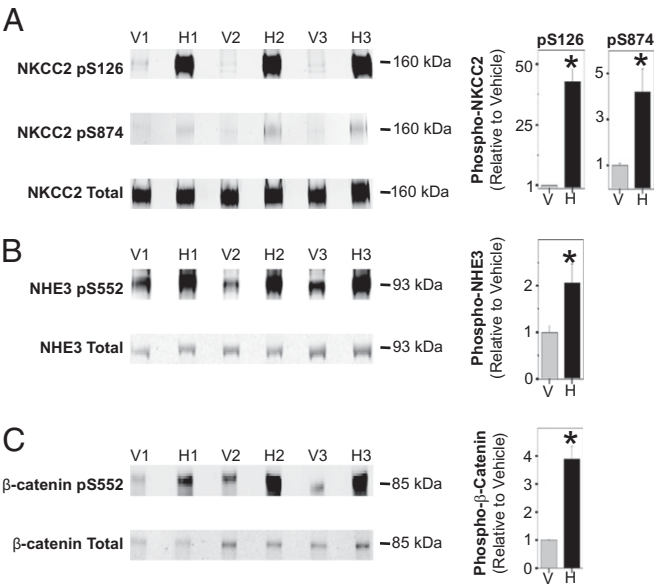

Fig. 4. Immunoblot confirmation of regulated sites. Immunoblotting with phospho-specific antibodies confirmed phosphorylation of NKCC2 at Ser126 (*A*, *Top*) and Ser874 (*A*, *Middle*), NHE3 at Ser552 (*B*, *Top*), and β-catenin at Ser552 (*C*, *Top*) in paired vehicle- and hormone-treated mTAL suspensions. In each case (*A*–*C*), the respective holo-protein was also probed. Bar graph shows results of densitometry analysis of immunoblots. H, hormone treated; V, vehicle. Error bars indicate SEM ($n = 3$). The asterisk indicates statistical significance ($P < 0.05$).

and/or CAMK families. A similar pattern was recently reported in cultured renal collecting duct cells in response to vasopressin (12). Previous studies in mTAL have concluded that at least one AGC kinase, namely PKA, plays a critical role in vasopressin-mediated signaling (13). A role for calmodulin-sensitive kinases has also been reported in the TAL (14). However, at least 105 protein kinases (including many AGC and CAMK family kinases) are known to be expressed in the rat mTAL (9), and roles for most of these have not been explored.

Majority of Sites at Which Phosphorylation Decreased Were Proline-Directed Sites. A proline-directed site has a proline in key positions surrounding the phosphorylated residue (usually at positions +1 and −2) that determine the site specificity of phosphorylation. This pattern suggests that cAMP-mediated signaling in the mTAL involves down-regulation of kinases in the MAPK (CMGC-II) and/or cyclin-dependent (CMGC-I) kinase families (7). A similar reduction in phosphorylation at proline-directed sites was recently reported in response to vasopressin in cultured renal collecting duct cells (12). Several publications have implicated MAP kinases in the regulation of various processes in TAL cells (15–17).

Regulated TAL Proteins Include Protein Phosphatase Regulators, Transmembrane Transporters, and Cytoskeletal Binding Proteins. Bioinformatic analysis using DAVID software allowed us to classify proteins by molecular function and other characteristics. Protein phosphatases stand with protein kinases as primary determinants of the phosphorylation state of any cell. Thus, the finding of selective changes in the phosphorylation of protein phosphatase regulators could provide an important clue to understanding TAL signaling. Previous studies have already implicated DARPP-32, the protein phosphatase 1 regulatory subunit, in TAL function (18). On the basis of studies in brain tissue, the phosphorylation site found in our study (Thr34) is believed to be a PKA target and to be necessary for the regulatory activity of the protein (19). Among the transmembrane transporters whose phosphorylation was found to be regulated by cAMP-increasing hormones was Glut4 (at Ser488), the insulin-dependent glucose carrier previously identified in the mTAL by Chin et al. (20). Studies in insulin-responsive tissues have implicated PKA in the phosphorylation of this site (21). Insulin is known to regulate Na^+ transport

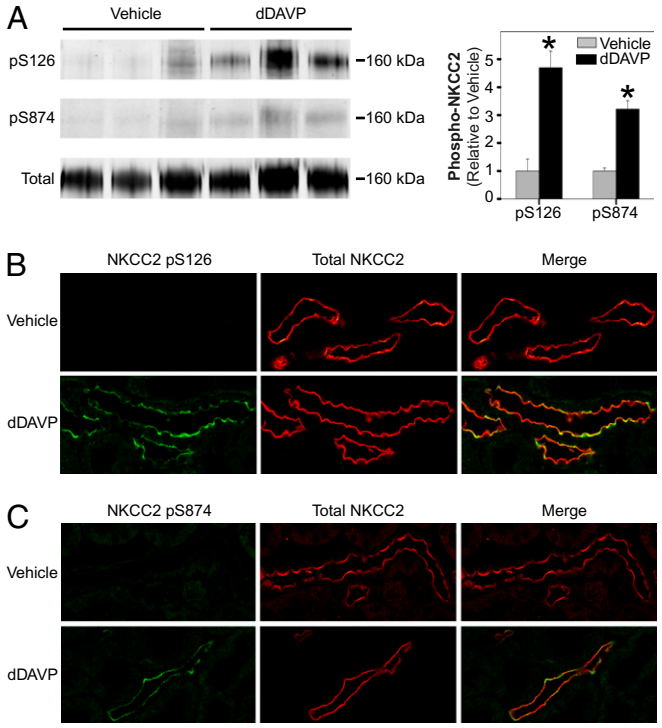

Fig. 5. Vasopressin effects on phosphorylation of NKCC2 in vivo. (*A*) Immunoblotting for NKCC2 phosphorylation at Ser126 (*Top*) and Ser874 (*Middle*) in outer medullary homogenates from vehicle- or dDAVP-treated Brattleboro rats. Total NKCC2 protein was also probed (*Bottom*). Bar graph shows results of densitometry analysis of immunoblots. Error bars indicate SEM (n = 3). Asterisks indicate statistical significance ($P < 0.05$). Immunolocalization of NKCC2 phosphorylated at Ser126 (*B*) and Ser874 (*C*) in perfusion-fixed kidneys from Brattleboro rats. Phospho-antibody, green; total NKCC2 antibody, red.

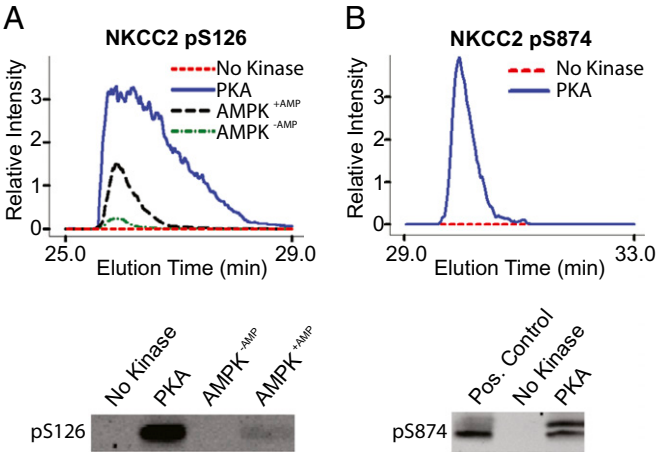

Fig. 6. Quantification of in vitro NKCC2 phosphorylation by PKA and AMPK. (*A*) Representative MS^1 time-course curves (*Upper*) quantifying phosphorylation of Ser126-containing peptide after incubation with purified PKA-α (blue) or AMPK-α2β1γ1 with (black) or without (green) 0.1 mM AMP. Immunoblotting confirmation (*Lower*) using pSer126-specific NKCC2 antibody. (*B*) Representative MS^1 time-course curves (*Upper*) quantifying phosphorylation of S874-containing peptide after incubation with purified PKA. Immunoblotting confirmation (*Lower*) using pSer874-specific NKCC2 antibody.

in the TAL (22), but its effect on glucose transport has not been studied to our knowledge. Aside from these regulated sites in transporters, potentially important phosphorylation sites were identified in several *Slc* family members, including anion exchanger 2 (*Slc4a2*), Na^+:H^+ exchanger 1 (*Slc9a1*), and lactate transporter MCT2 (*Slc16a7*).

Phosphorylation at Two Sites in the Na^+:K^+:2Cl^- Cotransporter NKCC2 (Ser126 and Ser874) Is Increased in Response to Vasopressin. NKCC2 is the primary transporter involved in apical NaCl transport in the mTAL. Both a previously unreported NKCC2 phosphorylation site at Ser874 and a known site at Ser126 (10) underwent strong increases in phosphorylation in response to vasopressin both in vitro and in vivo. Confocal immunofluoresence labeling of both phosphorylation sites showed a strong vasopressin response and supported previous observations that TAL cells are heterogeneous (23). In vitro phosphorylation assays showed that both sites can be phosphorylated by PKA, but roles for other basophilic kinases present in the mTAL cannot be excluded. Mutation of Ser126 to Ala was previously shown to decrease NKCC2 transport activity (10). There is evidence for a role for AMP-activated kinase in this phosphorylation (10), and AMPK did indeed relatively weakly phosphorylate this site in our in vitro assays.

Phosphorylation at Ser552 in the Na^+:H^+ Exchanger NHE3 Is Increased in Response to Vasopressin. Although Ser552 of NHE3 has been found to be phosphorylated in renal proximal tubule cells (24), this phosphorylation event has not been studied in the TAL to our knowledge. Here we have demonstrated a strong increase in phosphorylation at this site in response to the cAMP-generating hormone mixture or vasopressin alone. Studies by Kocinsky et al. (24) suggest that phosphorylation at Ser552 does not directly affect NHE3 activity but do not rule out a role in NHE3 trafficking.

Phosphorylation of Regulatory Proteins. Among the regulatory proteins whose phosphorylation state was altered are the phosphatase regulators described above and β-catenin, phosphorylated at a known PKA site, Ser552 (25). Phosphorylation at this site was increased by approximately fourfold in response to the cAMP-generating hormone mixture. This response is similar to what was found previously in inner medullary collecting duct suspensions (26) and cultured collecting duct cells in response to vasopressin (12). β-Catenin is a structural protein that binds to cadherins at adherens junctions and plays an additional role as a transcriptional coregulator in the Wnt signaling pathway.

In addition to phosphatase regulators and β-catenin, a number of other important regulatory proteins can be found in the general list of phosphorylation sites included in Table S1 and at http://dir.nhlbi.nih.gov/papers/lkem/mtalpd/. These include barttin, a protein that interacts with the basolateral chloride channel CLC-K2 and is mutated in one form of Bartter's syndrome (five phosphorylation sites) (27). Also included are the PDZ-domain proteins NHERF1 (four sites), Par-3 (1 site), and Shank2 (three sites) and kinase proteins such as the type II-α and -β regulatory subunits of PKA (both basophilic sites) and the STE20-like serine/threonine-protein kinase Slk. Finally, two sites were found on cystin, a recently characterized cilia-associated protein that is disrupted in the *cpk* mouse model of polycystic kidney disease (28).

Materials and Methods

Animals. All experiments were conducted in accord with animal protocol H-0110R1, which was approved by the Animal Care and Use Committee of the National Heart, Lung and Blood Institute.

mTAL Isolation, Hormone Treatment, and LC-MS/MS Analysis. Full methods are reported in *SI Materials and Methods*. Briefly, mTAL suspensions were prepared from outer medullas of Sprague-Dawley rats (Taconic Farms) using collagenase B/hyaluronidase treatment and low-speed centrifugation. Suspensions were incubated for 15 min with the vasopressin analog dDAVP (1 nM; Bachem), glucagon (100 nM; Sigma-Aldrich), parathyroid hormone (10 nM; Sigma-Aldrich), and calcitonin (1 μM; Sigma-Aldrich), either individually or in combination. Suspensions were preincubated for 15 min with phosphodiesterase inhibitor IBMX (0.5 mM; Sigma-Aldrich). LC-MS/MS analysis was carried out on an LTQ-Orbitrap system with collision-induced dissociation fragmentation after sample preparation that included extraction and denaturation of proteins, reduction/alkylation, in-solution trypsin digestion, and IMAC-based phospho-

peptide enrichment (29). (Note that, other than IMAC, we carried out no upstream fractionation to maximize the precision of the quantification, but at the expense of a lower number of phosphopeptide identifications that would otherwise be the case. This choice also reduced the possibility of systematic error related to differential effects on phosphopeptide isolation; e.g., during membrane fractionation.)

Data Repository. Mass spectrometric raw data have been deposited in the Tranche repository to facilitate data sharing and validation and can be downloaded at http://www.proteomecommons.org/ (*SI Materials and Methods*).

Computational Analysis. MS spectra were searched using three different search algorithms: InsPecT, SEQUEST, and OMSSA (*SI Materials and Methods*). Searches were conducted against the most recent *Rattus norvegicus* RefSeq Database (National Center for Biotechnology Information) using the target-decoy approach with filters adjusted to limit the false discovery rate to <2% as described in previous work (12). Quantification of relative phosphopeptide abundance (area under MS^1 time-course curve or extracted ion chromatogram elution profile) was implemented using QUOIL, an in-house software program designed for quantification of label-free peptides by LC-MS (30). Phosphorylation site assignment was performed using Ascore and PhosphoScore for SEQUEST data and the Phosphate Localization Score for InsPecT data (*SI Materials and Methods*). The open access web tool enoLOGOS (6) was used to generate weighted sequence logos from the aligned sequences of the up- and down-regulated phosphopeptides.

Short-Term dDAVP Treatment of Brattleboro Rats. Immunoblotting of outer medullary tissue from Brattleboro rats (Harland Sprague-Dawley) was performed as described in *SI Materials and Methods*. These rats were treated with a single injection of either dDAVP (2 nmol) or vehicle 1 h before euthanization.

In Vitro Kinase Assay. Nonphosphorylated peptides corresponding to the sequences surrounding Ser126 and Ser874 of rat NKCC2 were synthesized (AnaSpec). The sequence of the synthetic peptide for Ser126 contained amino acids 119–136 of rat NKCC2 (biotin-GPKVNRPSLQEIHEQLAK) and that for Ser874 contained amino acids 866–890 of rat NKCC2 (biotin-TKPAPKKDSNISTIQSMHVGEFNQK). Both peptides (0.4 nmol) were incubated with purified active PKA-α (*PRKACA*) or purified active AMPK-α2β1γ1 (with or without 0.1 mM AMP) at a kinase:peptide molar ratio of 1:32 in kinase reaction buffer supplemented with 200 μM ATP for 1 h at 37 °C (all components from Cell Signaling). The rat acetyl-CoA carboxylase derived SAMS peptide (biotin-HMRSAMSGLHLVKRR; Enzo Life Sciences) was used as an established substrate for AMPK phosphorylation (31).

Preadsorbed R5 NKCC2 Antibodies. Aliquots of the R5 antibody (gift from B. Forbush, Yale University, New Haven, CT), which detects phosphorylation at Thr(p)-96 and/or Thr(p)-101 in rat NKCC2 (11), were preadsorbed separately with synthetic peptides (AnaSpec) singly phosphorylated at either site to enable selective detection of phosphorylation at the unblocked phosphorylation site. The sequences of these synthetic phosphopeptides correspond to amino acids 92–107 (YYLRTFGHNTMDAVPR) in rat NKCC2, with monophosphorylation at either threonine. Preadsorption was carried out at an antibody:peptide molar ratio of 1:10 at 4 °C for 24 h.

Phospho-Specific NKCC2 Antibodies. Rabbit polyclonal phospho-specific NKCC2 antibodies recognizing Ser(p)-126 and Ser(p)-874 were generated against synthetic phosphopeptides and affinity purified (PhosphoSolutions) (*SI Materials and Methods*).

Other Antibodies. A rabbit polyclonal antibody (H7644) against total NHE3 was generated (Lofstrand Labs) against a synthetic peptide corresponding to amino acids 621–640 of rat NHE3 (RefSeq: NP_036786) and affinity purified (*SI Materials and Methods*).

ACKNOWLEDGMENTS. We thank Luke Xie, Ming-Jiun Yu, and Jae Song for assistance and advice. Mass spectrometry was conducted in the National Heart, Lung and Blood Institute Proteomics Core Facility (director, Marjan Gucek). Confocal fluorescence imaging was performed in the National Heart, Lung and Blood Institute Light Microscopy Core Facility (director, Christian Combs). This work was funded by the operating budget of Division of Intramural Research, National Heart, Lung and Blood Institute Project ZO1-HL001285 (to M.A.K.). M.M.R. was supported by the Braun Foundation (Melsungen, Germany) and the Biomedical Sciences Exchange Program (Hannover, Germany).

1. Kuhn W, Ramel A (1959) Active salt transport as possible (and probable) single effect in urine concentration in the kidney. *Helv Chim Acta*, 42:628–660 (in German).
2. Morel F, et al. (1982) Multiple hormonal control of adenylate cyclase in distal segments of the rat kidney. *Kidney Int Suppl* 11:S55–S62.
3. Knepper MA, Hoffert JD, Packer RK, Fenton RA (2008) *Brenner & Rector's The Kidney*, ed Brenner B (Saunders Elsevier, Philadelphia), pp 308–329.
4. Knepper MA, Danielson RA, Saidel GM, Post RS (1977) Quantitative analysis of renal medullary anatomy in rats and rabbits. *Kidney Int* 12:313–323.
5. Elias JE, Gygi SP (2007) Target-decoy search strategy for increased confidence in large-scale protein identifications by mass spectrometry. *Nat Methods* 4:207–214.
6. Workman CT, et al. (2005) enoLOGOS: A versatile web tool for energy normalized sequence logos. *Nucleic Acids Res* 33 (Web Server issue):W389–W392.
7. Miller ML, et al. (2008) Linear motif atlas for phosphorylation-dependent signaling. *Sci Signal* 1:ra2.
8. Huang W, Sherman BT, Lempicki RA (2009) Systematic and integrative analysis of large gene lists using DAVID bioinformatics resources. *Nat Protoc* 4:44–57.
9. Yu MJ, et al. (2009) Systems-level analysis of cell-specific AQP2 gene expression in renal collecting duct. *Proc Natl Acad Sci USA* 106:2441–2446.
10. Fraser SA, et al. (2007) Regulation of the renal-specific Na^+-K^+-$2Cl^-$ co-transporter NKCC2 by AMP-activated protein kinase (AMPK). *Biochem J* 405:85–93.
11. Flemmer AW, Gimenez I, Dowd BF, Darman RB, Forbush B (2002) Activation of the Na-K-Cl cotransporter NKCC1 detected with a phospho-specific antibody. *J Biol Chem* 277:37551–37558.
12. Rinschen MM, et al. (2010) Quantitative phosphoproteomic analysis reveals vasopressin V2-receptor-dependent signaling pathways in renal collecting duct cells. *Proc Natl Acad Sci USA* 107:3882–3887.
13. Edwards RM, Jackson BA, Dousa TP (1980) Protein kinase activity in isolated tubules of rat renal medulla. *Am J Physiol* 238:F269–F278.
14. Kinne-Saffran E, Kinne RK (1997) Sorbitol uptake in plasma membrane vesicles isolated from immortalized rabbit TALH cells: Activation by a Ca^{2+}/calmodulin-dependent protein kinase. *J Membr Biol* 159:231–238.
15. Watts BA, III, Di Mari JF, Davis RJ, Good DW (1998) Hypertonicity activates MAP kinases and inhibits HCO_3 absorption via distinct pathways in thick ascending limb. *Am J Physiol* 275:F478–F486.
16. Gallazzini M, Karim Z, Bichara M (2006) Regulation of ROMK (Kir 1.1) channel expression in kidney thick ascending limb by hypertonicity: Role of TonEBP and MAPK pathways. *Nephron, Physiol* 104:126–135.
17. Roger F, Martin PY, Rousselot M, Favre H, Féraille E (1999) Cell shrinkage triggers the activation of mitogen-activated protein kinases by hypertonicity in the rat kidney medullary thick ascending limb of the Henle's loop. Requirement of p38 kinase for the regulatory volume increase response. *J Biol Chem* 274:34103–34110.
18. Fryckstedt J, Meister B, Aperia A (1992) Control of electrolyte transport in the kidney through a dopamine- and cAMP-regulated phosphoprotein, DARPP-32. *J Auton Pharmacol* 12:183–189.
19. Williams KR, Hemmings HC, Jr, LoPresti MB, Konigsberg WH, Greengard P (1986) DARPP-32, a dopamine- and cyclic AMP-regulated neuronal phosphoprotein. Primary structure and homology with protein phosphatase inhibitor-1. *J Biol Chem* 261: 1890–1903.
20. Chin E, Zhou J, Bondy C (1993) Anatomical and developmental patterns of facilitative glucose transporter gene expression in the rat kidney. *J Clin Invest* 91:1810–1815.
21. Michelle Furtado L, Poon V, Klip A (2003) GLUT4 activation: Thoughts on possible mechanisms. *Acta Physiol Scand* 178:287–296.
22. Ito O, et al. (1994) Insulin stimulates NaCl transport in isolated perfused MTAL of Henle's loop of rabbit kidney. *Am J Physiol* 267:F265–F270.
23. Allen F, Tisher CC (1976) Morphology of the ascending thick limb of Henle. *Kidney Int* 9:8–22.
24. Kocinsky HS, Dynia DW, Wang T, Aronson PS (2007) NHE3 phosphorylation at serines 552 and 605 does not directly affect NHE3 activity. *Am J Physiol Renal Physiol* 293: F212–F218.
25. Taurin S, Sandbo N, Qin Y, Browning D, Dulin NO (2006) Phosphorylation of β-catenin by cyclic AMP-dependent protein kinase. *J Biol Chem* 281:9971–9976.
26. Bansal AD, et al. (2010) Phosphoproteomic profiling reveals vasopressin-regulated phosphorylation sites in collecting duct. *J Am Soc Nephrol* 21:303–315.
27. Estévez R, et al. (2001) Barttin is a Cl- channel beta-subunit crucial for renal Cl- reabsorption and inner ear K^+ secretion. *Nature* 414:558–561.
28. Hou X, et al. (2002) Cystin, a novel cilia-associated protein, is disrupted in the *cpk* mouse model of polycystic kidney disease. *J Clin Invest* 109:533–540.
29. Hoffert JD, Pisitkun T, Wang G, Shen RF, Knepper MA (2006) Quantitative phosphoproteomics of vasopressin-sensitive renal cells: Regulation of aquaporin-2 phosphorylation at two sites. *Proc Natl Acad Sci USA* 103:7159–7164.
30. Wang G, Wu WW, Zeng W, Chou CL, Shen RF (2006) Label-free protein quantification using LC-coupled ion trap or FT mass spectrometry: Reproducibility, linearity, and application with complex proteomes. *J Proteome Res* 5:1214–1223.
31. Sullivan JE, Carey F, Carling D, Beri RK (1994) Characterisation of 5′-AMP-activated protein kinase in human liver using specific peptide substrates and the effects of 5′-AMP analogues on enzyme activity. *Biochem Biophys Res Commun* 200:1551–1556.